

Electrochemical enhancement of adsorption capacity of activated carbon fibers and their surface physicochemical characterizations

Yanhe Han, Xie Quan^{*}, Shuo Chen, Shibo Wang, Yaobin Zhang

School of Environmental and Biological Science & Technology, Dalian University of Technology, Key Laboratory of Industrial Ecology and Environmental Engineering, Ministry of Education, Linggong Road 2#, Dalian 116023, China

Received 19 May 2006; received in revised form 21 September 2006; accepted 21 September 2006

Available online 23 October 2006

Abstract

The adsorption of activated carbon fibers (ACFs) and their surface characteristics were investigated before and after electrochemical polarization. The adsorption kinetics of *m*-cresol showed the dependence on polarized potential, and the adsorption rate constant increased by 77.1%, from $6.38 \times 10^{-3} \text{ min}^{-1}$ at open-circuit (OC) to $1.13 \times 10^{-2} \text{ min}^{-1}$ at polarization of 600 mV. The adsorption isotherms at different potentials were in good agreement with Langmuir isotherm model, and the maximum adsorption capacity increased from 2.28 mmol g^{-1} at OC to 3.67 mmol g^{-1} at polarized potential of 600 mV. These indicated that electrochemical polarization could effectively improve the adsorption rate and capacity of ACFs. The surface characteristics of ACFs before and after electrochemical polarization were evaluated by N_2 adsorption–desorption isotherms, scanning electron microscope (SEM), zeta potential and Fourier transform infrared spectroscopy (FTIR). The results showed that the BET specific surface area and pore size increased as the potential rose. However, the surface chemical properties of ACFs hardly changed under electrochemical polarization of less than 600 mV. This study was beneficial to understand the mechanism of electrochemically enhanced adsorption.

© 2006 Elsevier Ltd. All rights reserved.

Keywords: Electrosorption; Adsorption kinetics; Adsorption isotherms; Activated carbon fibers; Surface properties

1. Introduction

Electrochemistry is widely used in wastewater treatment because of its environmentally friendly advantage. Electrochemical treatment technologies include electro-oxidation [1–3], electro-reduction [4–8] and electrosorption [9–15]. Electro-oxidation and reduction are Faraday processes containing charge transfer through the phase boundary. However, electrosorption, which is generally defined as potential polarization-induced adsorption on the surface of electrodes, is a non-Faraday process. After the polarization of the electrodes, the polar molecules or ions can be removed from the electrolyte solution by the imposed electric field and adsorbed onto the surface of the electrodes. Because of its low energy consumption and environmentally friendly advantage, electrosorption has attracted a wide interest in the adsorption processes for the treatment of wastewater and the purification of supplying water. The investigations suggest

that electrosorption can effectively enhance the adsorption of metal ions. The electrosorption processes of ions are mature, and the corresponding industrial products have been developed.

However, the electrosorption for organic substances is a new technology. Some researchers [16–21] are exploring the feasibility of electrosorption for organic substances. Plaisance et al. [16] found that the 34% enhancement of adsorption capacity for benzene by electrochemical polarization was achievable. Niu and Conway [21] reported that the polarization of C-electrodes could enhance the adsorption rate of pyridinium ion, 1,4-pyrazine and 1-quinoline in the wastewater. These investigations indicate that electrochemical polarization can enhance adsorption rate and efficiency of organic substances on C-electrodes.

The capacity and rate of adsorption for porous materials depend on many factors, such as the nature of pore structure and the surface polarity [13]. It is well known that the surface area and pore size distribution of adsorbents play an important role during the adsorption processes. Besides the surface chemical properties and the interaction affinity between adsorbates and adsorbents, the surface area and the pore size distribution may be also affected by electrochemical polarization.

^{*} Corresponding author. Tel.: +86 411 84706140; fax: +86 411 847 6263.
E-mail address: quanxie@dlut.edu.cn (X. Quan).

Therefore, to understand the mechanism of the enhancement for the adsorption rate and capacity of activated carbon fibers (ACFs), the investigation of physical and chemical properties of adsorbents after electrochemical polarization is important. However, to the best of our knowledge, the investigation of characteristics for activated carbon after electrochemical polarization has not been found.

The objective of this study is to investigate the effects of electrochemical polarization on the adsorption rate and capacity of ACFs. And the physiochemical properties of ACFs, such as BET surface area, pore size distribution, the surface morphologies, zeta potential and surface functional groups, were analyzed to better understand the mechanism of electrosorption. We selected *m*-cresol as target substance, which is one kind of noxious organic pollutants that is present in some industrial wastewaters and needs to be removed, to study its electrosorption rate and capacity on ACFs electrode.

2. Experimental

2.1. Pretreatment of ACFs

The commercial polyacrylonitrile-based ACFs cloth (obtained from Anshan Activated Carbon Fiber Company, China) were first heated in boiling 5% NaOH for 1 h, which may avoid the desorption of trace organic compounds during the adsorption procedure. And then the ACFs seethed in 5% HCl for 1 h after a batch of deionization elution procedures was applied, which remove fines and inorganic ions that may dissolve during the adsorption measurements. At last, the ACFs treated by the above procedures was heated in boiling deionized water for 1 h, immersed overnight in the deionized water and washed to neutral. Then the washed ACFs was dried at 105 °C for 24 h [22], and kept in a desiccator for use.

2.2. Characterization of ACFs

The BET surface area and pore size distribution of ACFs before and after electrochemical polarization in the solution of 0.01 mol L⁻¹ Na₂SO₄ were carried out with an automated gas sorption system, using N₂ as the adsorbate at 77 K. Before the experiment, the ACFs were heated at 100 °C and outgassed to a vacuum of around 10⁻⁵ Torr. The pore size was calculated using the BJH model in the range 2.0–100 nm.

The surface morphologies of ACFs before and after electrochemical polarization were characterized by scanning electron microscopy (SEM, JSM-5600LV, Oxford, UK) with an accelerating voltage of 20 kV. The zero-potentials were measured by a Zetameter (Zetaplus V3.52, Japan). Six solutions of 50 mg L⁻¹ of each ACFs ground after different polarization were prepared in bottles with CO₂-free bi-distilled water with 1 mmol L⁻¹ KCl. The pH value was adjusted between 2 and 12 by adding HCl and NaOH. The bottles were sealed, dispersed uniformly by ultrasonic treatment for 24 h and left to stabilize for 24 h before the measurements. The Fourier transform infrared spectroscopy (FTIR) analysis was performed after grinding the carbon samples and mixing with KBr power to prepare sample-KBr pellets.

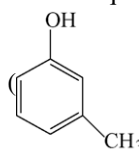
The infrared spectra of ACFs were recorded at room temperature in the range between 400 and 4000 cm⁻¹ using a Fourier transform spectrophotometer (IR Prestige-21, Shimadzu, Japan). Pellets thickness was kept constant by fixing the sample-in-KBr weight (180 ± 0.2 mg), using the same die diameter, being palletized under the same pressure and time. The ACFs contained in the pellets was 0.1 wt%.

2.3. Instrumentation and adsorption cell

A conventional three-dimensional electrode system was adopted in the adsorption/electrosorption investigation in both open-circuit (OC) and electrochemical polarization experiments. The experimental apparatus was in detail described in our previous work [23]. All experiments were performed with a CH Instruments Model 800A electrochemical workstation (Shanghai Chenhua Corporation, China) for supplying bias potential, which was connected with a personal computer that was used to control the experimental parameters. The working electrode was a piece of ACFs (weight 30.0 ± 0.5 mg) connected by platinum wire, which was fixed by plexiglas with four big holes. Saturated calomel electrode (SCE) was selected as the reference electrode, and the distance between SCE and the working electrode was about 2.5 mm. The auxiliary electrode, a piece of platinum plate (25 mm × 25 mm) attached to another platinum wire, served as a current collector. And the distance between the working electrode and counter electrode was 45 mm.

2.4. Adsorption/electrosorption kinetics

The adsorption/electrosorption kinetics experiments were carried out in the aqueous solution of 100 mL with 2 mmol L⁻¹

m-cresol () and 0.01 mol L⁻¹ Na₂SO₄. The 1 mL

solution was withdrawn at a given time intervals, diluted to 10 mL with deionized water and the concentration was measured by UV–vis spectrophotometer (JASCO V-550, Japan) at 271 nm. The adsorption rate constants of *m*-cresol were determined with the Lagergren [24] Eq. (1), which is the first-order adsorption kinetics equation:

$$\log(q_e - q) = \log q_e - \frac{k_{\text{ads}} t}{2.303} \quad (1)$$

where k_{ads} (min⁻¹) is the adsorption rate constant, q_e and q (mmol g⁻¹) are the amounts of *m*-cresol adsorbed at equilibrium and time t (min), respectively.

2.5. Adsorption/electrosorption isotherms

Isotherm experiments for *m*-cresol at different bias potentials, corresponding to adsorption/electrosorption kinetics, were carried out with fixed amount of ACFs (30.0 ± 0.5 mg). The amount of adsorbed *m*-cresol was calculated from the following

equation:

$$q_e = \frac{(C_0 - C)V}{m} \quad (2)$$

where C_0 and C are the concentration at the beginning and the equilibrium adsorption state, respectively. V is the volume of solution and m is the mass of ACFs. Isotherms in all experimental cases were fitted to two classical empirical models of Langmuir [25] and Freundlich [26].

$$q_e = Q_L \frac{b_L C_e}{1 + b_L C_e} \quad (3)$$

$$q_e = k_F C_e^{1/n} \quad (4)$$

where Q_L is the maximum saturation adsorption capacity, b_L the Langmuir constant, K_F and n are the Freundlich constants.

3. Results and discussion

3.1. The determination of electrosorption potential window for *m*-cresol

In order to ensure that the *m*-cresol was not oxidized or reduced during the electrosorption process, the electrosorptive bias potential must be controlled. The cyclic voltammetries of solution without and with *m*-cresol were measured by electrochemical workstation at anodic polarization, respectively, and the results are shown in Fig. 1. Steady increases and decreases observed in current with electric potential in both solutions indicate that no oxidation or reduction occurs in the range between 0 and 600 mV. Therefore, the electrosorption was carried out in this potential range to prevent *m*-cresol from being reduced or oxidized.

3.2. Adsorption/electrosorption kinetics

To investigate the effect of electrochemical polarization on the adsorption rate which is necessary for the accurate design

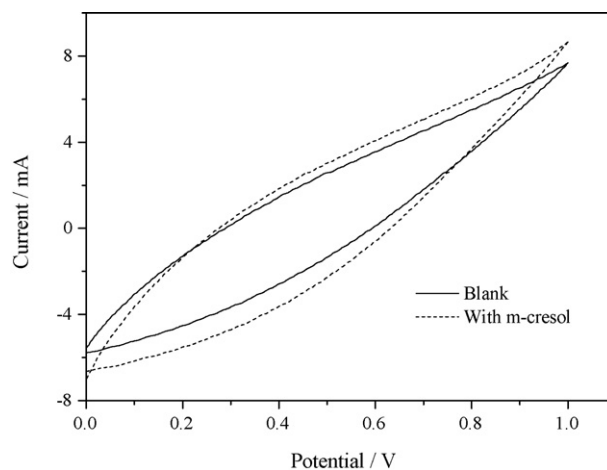


Fig. 1. The cyclic voltammetries of 30 mg ACFs in 0.01 mol L⁻¹ Na₂SO₄ solution without and with *m*-cresol at scan rate of 5 mV S⁻¹.

and model of adsorption processes, four experiments on adsorption/electrosorption kinetics were carried out with the initial *m*-cresol concentration of about 2 mmol L⁻¹, the ACFs weight of 30 mg, at room temperature, but at different bias potentials (OC, 200, 400 and 600 mV). The adsorption rate constants were determined using Lagergren adsorption kinetics equation and were found to be 6.38×10^{-3} , 8.56×10^{-3} , 1.14×10^{-2} and 1.13×10^{-2} min⁻¹ at the polarization of OC, 200, 400 and 600 mV, respectively. The results (shown in Fig. 2) show that the adsorption rate constants and capacity are improved with increasing the bias potential of electrochemical polarization, indicating that electrochemical polarization can effectively enhance the adsorption rate and capacity of *m*-cresol on ACFs. The pH almost remained constant during the course of all experiments, suggesting that water splitting didn't happen. According to the results of cyclic voltammetry, electrochemical degradation of *m*-cresol was unable to happen when bias potential supplied was below 600 mV. This implies that the enhancement of adsorption rate and capacity for *m*-cresol at bias potentials supplied is not due to direct electrochemical degradation or secondary

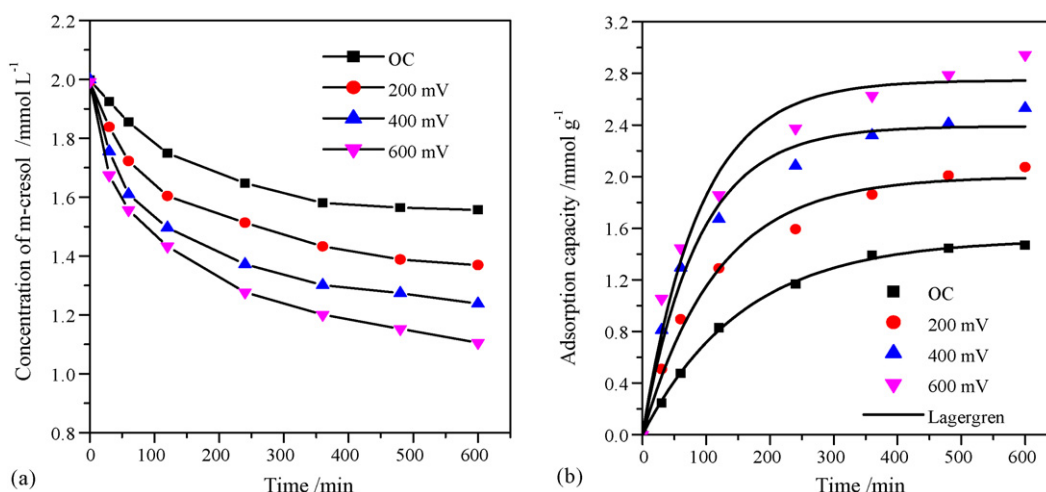


Fig. 2. The adsorption/electrosorption kinetics of *m*-cresol on 30 mg ACFs with the initial concentration of 2 mmol L⁻¹ and 0.01 mol L⁻¹ Na₂SO₄. (a) Concentration vs. time curve, (b) corresponding adsorption capacity vs. time curve. Solid line in (b) represents the simulation data based on the first-order adsorption kinetics.

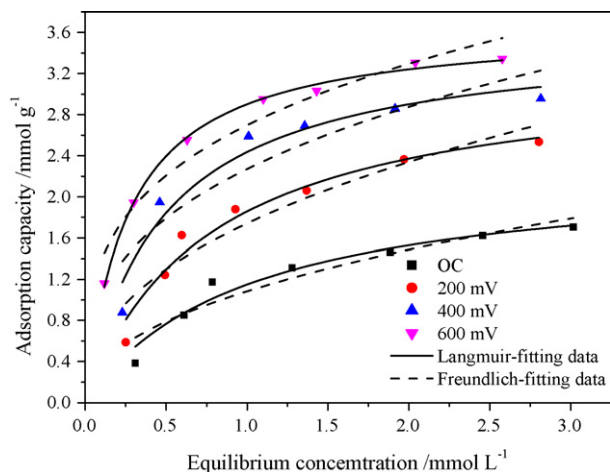


Fig. 3. The adsorption isotherms of *m*-cresol in 0.01 mol L⁻¹ Na₂SO₄ solution at different potentials with temperature 25 °C.

reactions caused by active oxidizing free radicals, such as free hydroxyl radicals produced by electrochemical water splitting, but may mainly be due to the affinity between the surface of ACFs and *m*-cresol, enhanced by the polarization under electric field.

3.3. Adsorption/electrosorption isotherms

The adsorption capacity of adsorbents is a very important parameter in the practical process design. Therefore, the adsorption isotherms at different bias potentials, OC, 200, 400 and 600 mV, corresponding to the polarization potentials for kinetics above-mentioned, were investigated at 25 °C for 22 h. Fig. 3 shows the experimental equilibrium data and corresponding ones fitted with the Langmuir and Freundlich isotherms. The results show that the adsorption capacity of *m*-cresol enhances with increasing polarization potential, indicating that the adsorption capacity of ACFs can be effectively improved by electrochemical polarization. The parameters for two isotherms were evaluated by least squares method based on an optimization algorithm and shown in Table 1 along with the average absolute percentage deviation, %D, which is determined as follows:

$$\%D = \left(\frac{1}{N} \sum_{i=1}^N \left| \frac{q_{\text{exp}} - q_{\text{pred}}}{q_{\text{exp}}} \right| \right) \times 100\% \quad (5)$$

where N is the number of experimental data points, q_{pred} (mmol g⁻¹) the predicted amount of *m*-cresol adsorbed with the isotherm model and q_{exp} (mmol g⁻¹) is the experimental

Table 1
Langmuir and Freundlich isotherms constants at 25 °C

Potential (mV)	Langmuir				Freundlich			
	Q_L	b_L	R^2	%D	K_F	$1/n$	R^2	%D
OC	2.28	1.01	0.958	8.9	1.08	0.46	0.906	14.0
200	3.28	1.31	0.964	8.7	1.74	0.43	0.902	14.7
400	3.58	2.12	0.951	9.0	2.27	0.34	0.843	16.0
600	3.67	3.76	0.997	1.2	2.70	0.29	0.948	7.0

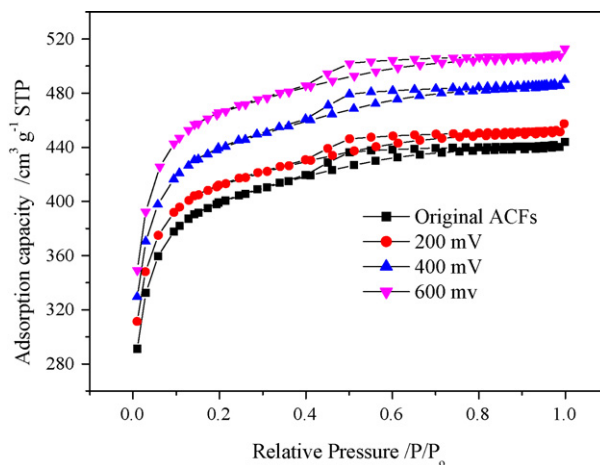


Fig. 4. N₂ adsorption-desorption isotherms of ACFs before and after different polarized potentials.

amount of *m*-cresol adsorbed. The experimental data is in good agreement with Langmuir with small percentage deviations and high correlation coefficient, suggesting that the adsorption of *m*-cresol at polarization is monolayer. And the b_L increases as the potential supplied rose from OC to 600 mV, showing that the affinity force can be effectively enhanced by electrochemical polarization. The maximum adsorption capacity increases by 61.0%, from 2.28 mmol g⁻¹ at OC to 3.67 mmol g⁻¹ at 600 mV.

3.4. The characterization of ACFs before and after electrochemical polarization

In order to understand the mechanism of electrosorption for *m*-cresol on ACFs, the surface characteristics of ACFs before and after electrochemical polarization were evaluated in this paper. The electrosorption was mainly monolayer that was mostly dependent on the BET surface area and the pore size distribution of adsorbent. Hence, the surface area and pore size distribution of ACFs before and after electrochemical polarization were investigated by N₂ adsorption. And the morphologies, zeta potential and surface functional groups were also investigated.

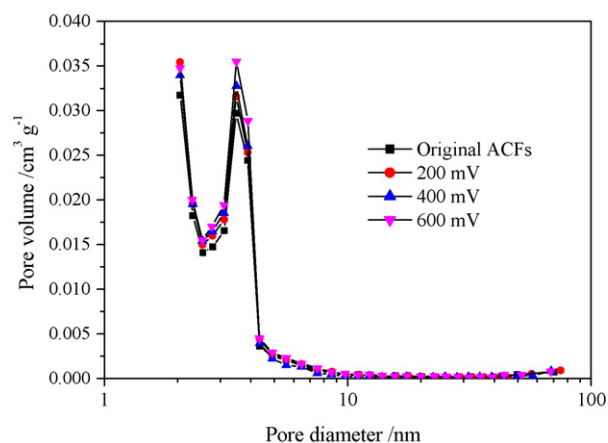


Fig. 5. Pore size distribution of ACFs before and after different polarized potentials.

3.4.1. The BET surface area and pore size distribution

The adsorption–desorption isotherms of N_2 on the ACFs were shown in Fig. 4. Based on their shape, the adsorption–desorption isotherms of ACFs before and after electrochemical polarization are type I according to the BDDT classification [27]. All of the isotherms have two characteristic regions; one below the relative pressure ($P/P_0 < 0.2$), where a rapid increase of adsorption uptake is observed with increasing P/P_0 . This indicates that the ACFs contain a large number of micropores. The appearance of hysteresis loops in the N_2 isotherms of all the ACFs indi-

cates the existence of some mesoporosity [28]. The hysteresis loops, whose area were 45.0, 46.9, 49.7 and 53.2, corresponding to the initial, 200, 400 and 600 mV polarized ACFs, increase slightly with increasing polarized potential. This suggests that the mesoporosity is enhanced slightly, which is also indicated by the later average pores. The BET surface areas of ACFs are 1335, 1384, 1479 and 1561 $m^2 g^{-1}$, corresponding to the initial, 200, 400 and 600 mV polarized ACFs, indicating that the electrochemical polarization can improve the BET surface areas. Only the inelastic deformation of surface, which was caused by

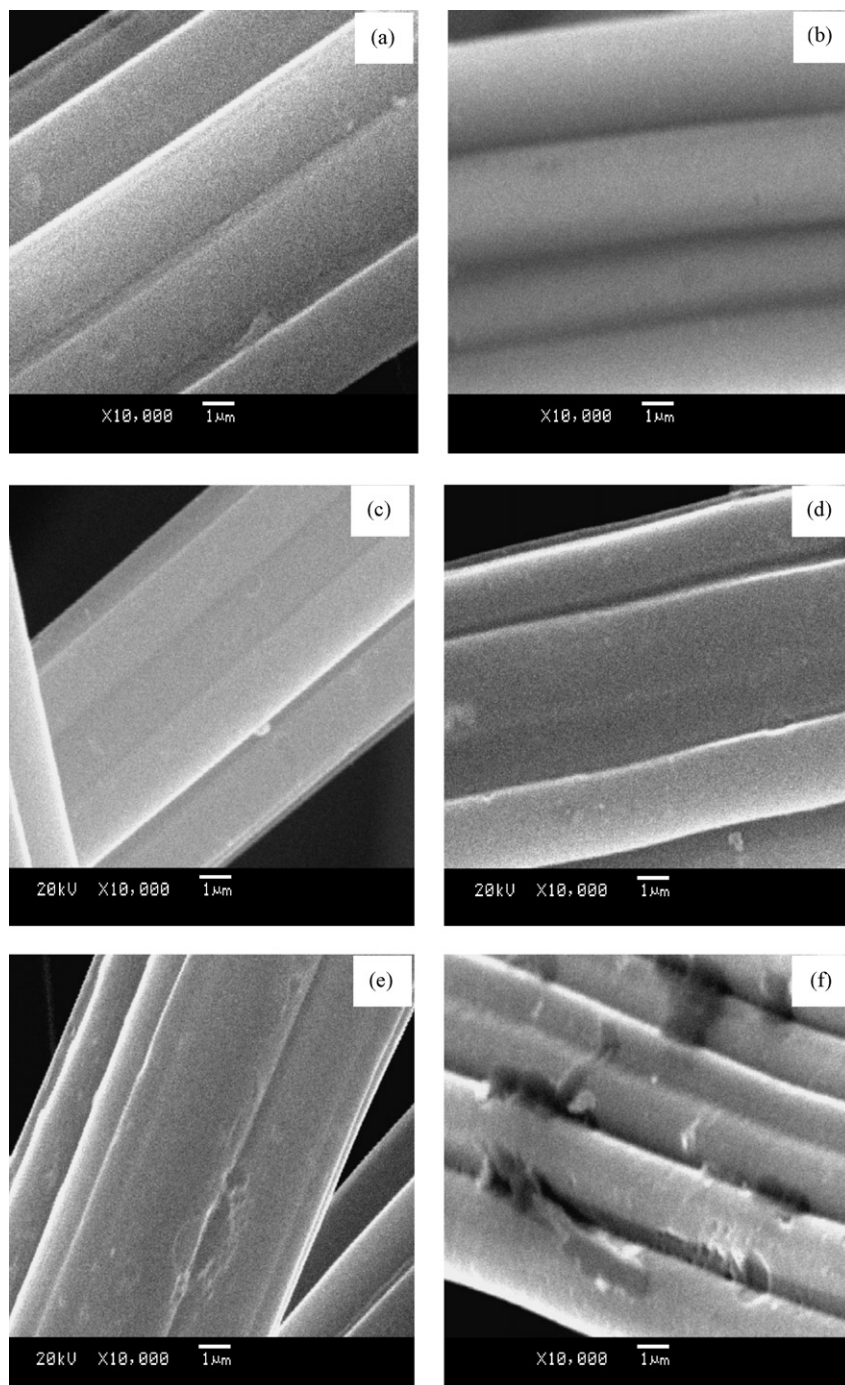


Fig. 6. Scanning electron micrographs of the ACFs: (a) initial surface, (b)–(f) after polarizing at 200, 400, 600, 800 and 1000 mV, respectively.

electrostatic repulsion and the expanded action of the adsorption enhanced under electrochemical polarization for water and adsorbates, can be measured by this measured method applied. It is well known that the specific surface area is an important factor affecting the monolayer adsorption capacity, which the higher BET surface area causes the higher adsorption capacity. The pore size distributions of ACFs calculated using BJH method were shown in Fig. 5 in the range 2–100 nm. It seems that the pores in the mesopore range, which are defined as pores of width between 2 and 50 nm, increase with the increasing potential in the experimental potential range. The mesopores contribution to the BET surface area of ACFs is usually smaller compared with micropores. However, they play an important role in the adsorption of organics [29]. Similar to the specific surface area measurement, only the inelastic deformation of pore size caused by electrochemical polarization can be measured by this measured method applied. The enhancement of adsorption capacity for *m*-cresol may mainly be due to the improvement of BET surface areas and average pore sizes besides the affinity between the surface of ACFs and *m*-cresol, enhanced by the polarization under electric field.

3.4.2. The surface morphologies

The surface morphologies of ACFs before and after polarization were characterized by SEM and shown in Fig. 6. In order to distinguish the morphologies of ACFs at different polarized potentials, the micrographs at the polarized potentials of 800 and 1000 mV were also shown. When the polarized potential is less than 600 mV, there is no evident difference in the surface of ACFs. When the polarized potential is over 800 mV, some pits are formed on the surface, indicating that the surface is electro-oxidized. Active oxidizing free radicals probably develop on the surface, which may oxidize the adsorbate during the electrosorption. Therefore, controlling the polarized potentials in the range between 0 and 600 mV is reasonable for the electrosorption of *m*-cresol.

3.4.3. The zeta potential

The zeta potential can represent a characteristic and practical value for the prevailing functional groups containing oxygen on the surface of ACFs [30]. By means of zeta potential measurements, valuable information can be obtained on the change that occurs on the surface of ACFs after electrochemical polarization. Fig. 7 shows the zeta potential of the ACFs before and after electrochemical polarization in the presence of 1 mmol L^{-1} KCl solution as a function of the pH value. With increasing pH value of the solution, the excess of negative charges on the surface of the ACFs increases. The isoelectric points (IEP, it is the pH at which the zeta potential is zero) of as received ACFs and the ACFs after polarizing at 200, 400 and 600 mV, are almost identical for the pH value of 6.1. However, the IEP is 5.0 in case of the polarization of 800 mV. This indicates that the surface functional groups are not affected by the electrochemical polarization in the range between 0 and 600 mV. There are more acidic functional groups [30] on the surface of ACFs after polarization of 800 mV, which may be resulted in by electrochemical oxidation. This is consistent with the results of SEM micrographs.

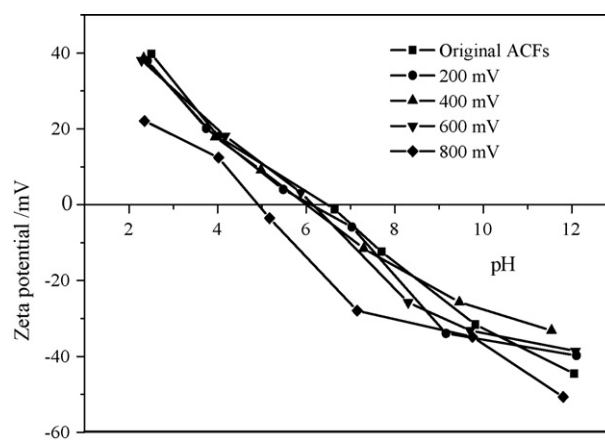


Fig. 7. Zeta potential of original and polarized ACFs as a function of pH in the presence of KCl (1 mmol L^{-1}).

3.4.4. FTIR

It is generally accepted that electrochemical polarization can change the surface oxygen-containing functional groups of ACFs. In order to investigate the change of surface functional groups, FTIR is used to qualitatively identify the functional groups of ACFs. The surface functional groups of the original and electrochemically polarized ACFs were evaluated by FTIR and the spectra are shown in Fig. 8. The results show that when the polarization potentials are less than 600 mV, there is no evident difference between original and polarized ACFs. However, new (3150 , 1300 – 1000 cm^{-1}) and higher relative intensities bands (1400 cm^{-1}) occur in the FTIR spectra for the ACFs at polarized potential of 800 mV. In spite of the fact that the measurement procedure applied here makes quantitative comparison of the FTIR spectra impossible, the presence and relative intensities of the respective bands indicate that some changes have occurred in the surface chemical structure of ACFs. The new band at around 3150 cm^{-1} is present, which may be assigned to the stretching vibration of $\text{O}-\text{H} \cdots \text{O}$ formed on the surface [31,32]. The band in the region of 1400 cm^{-1} , which was intensified after the polarization of 800 mV, can be ascribed to

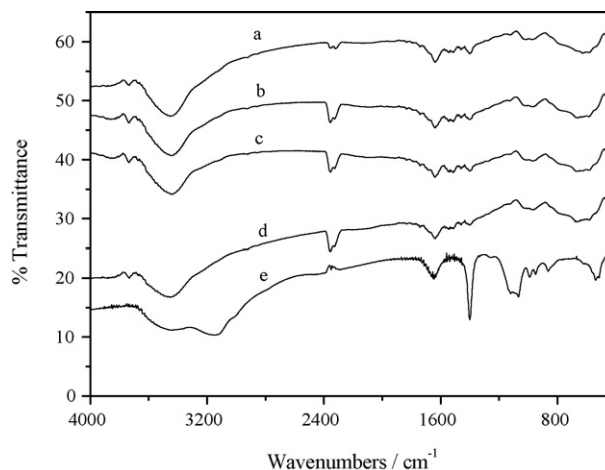


Fig. 8. FTIR spectra of ACFs before (a) and after polarization at 200 (b), 400 (c), 600 (d) and 800 mV (e).

carboxyl-carbonate structures [33]. The broad absorption within the range 1300–1000 cm⁻¹ can be assigned to various C–O bonds, such as those in ethers, phenols and hydroxyl groups [34]. Therefore, the surface of ACFs is probably oxidized at the polarization of 800 mV, but not at 600 mV, which is consistent with the results of SEM and zeta potential.

4. Conclusions

In a summary, the electrochemical polarization can effectively enhance the adsorption rate and capacity of ACFs for *m*-cresol. In all experimental cases, the adsorption kinetics is fitted to the first-order adsorption kinetics. The adsorption isotherms obtained for *m*-cresol at different potentials follow Langmuir isotherm model. And the maximum adsorption capacity increases by 61.0%, from 2.28 mmol g⁻¹ at OC to 3.67 mmol g⁻¹ at 600 mV. The ACFs before and after polarization were characterized by BET, SEM, zeta potential and FTIR. The BET results show that the surface area and average pore size increase with increasing the polarized potential. The results of the other characteristics suggest that the surface of ACFs is not oxidized when the potential applied is less than 600 mV. Therefore, the enhancement of surface area and pore size for ACFs probably plays an important role during the electrochemically enhanced adsorption process, being beneficial to understand the enhanced adsorption mechanism.

Acknowledgments

The authors would like to thank National Nature Science Foundation of China (No. 20337020) and National Basic Research Program of China (No. 2003CB415006) for financial support.

References

- [1] L.C. Chiang, J.E. Chang, T.C. Wen, *Water Res.* 29 (1995) 671.
- [2] M. Panizza, G. Cerisola, *Electrochim. Acta* 48 (2003) 1515.
- [3] P. Cañizares, J. Lobato, R. Paz, M.A. Rodrigo, C. Sáez, *Water Res.* 39 (2005) 2687.
- [4] M.S. Mubarak, D.G. Peters, *J. Electroanal. Chem.* 425 (1997) 13.
- [5] A. Matsunaga, A. Yasuhara, *Environ. Sci. Technol.* 37 (2003) 3435.
- [6] I.F. Cheng, Q. Fernando, N. Korte, *Environ. Sci. Technol.* 31 (1997) 1074.
- [7] H. Cheng, K. Scott, P.A. Christensen, *J. Electrochem. Soc.* 150 (2003) 17.
- [8] G. Chen, Z.Y. Wang, D.G. Xia, *Electrochim. Acta* 50 (2004) 933.
- [9] B.A. Bill, W.M. George, *J. Phys. Chem.* 65 (1961) 135.
- [10] K.L. Yang, T.Y. Ying, S. Yiacoumi, C. Tsouris, E.S. Vittoratos, *Langmuir* 17 (2001) 1961.
- [11] C.J. Gabelich, T.D. Tran, I.H. Suffet, *Environ. Sci. Technol.* 36 (2002) 3010.
- [12] A. Afkhami, B.E. Conway, *J. Colloid Interf. Sci.* 251 (2002) 248.
- [13] S.J. Park, B.J. Park, S.K. Ryu, *Carbon* 37 (1999) 1223.
- [14] J.S. Kim, C.H. Jung, W.Z. Oh, S.K. Ryu, *Carbon Sci.* 3 (2002) 6.
- [15] H.Y. Lee, C.H. Jung, W.Z. Oh, J.H. Park, Y.G. Shul, *Carbon Sci.* 4 (2003) 64.
- [16] H. Plaisance, P. Mocho, G. Bonnetaze, *Environ. Technol.* 17 (1996) 1313.
- [17] B.E. Conway, E. Ayranci, H. Al-Maznai, *Electrochim. Acta* 47 (2001) 705.
- [18] M.A. Tsvetnov, V.V. Khabalov, N.B. Kondrikov, *Colloid J.* 63 (2001) 248.
- [19] A. Bán, A. Schäfer, H. Wendt, *J. Appl. Electrochem.* 28 (1998) 227.
- [20] J.J. Niu, B.E. Conway, *J. Electroanal. Chem.* 546 (2003) 59.
- [21] J.J. Niu, B.E. Conway, *J. Electroanal. Chem.* 529 (2002) 84.
- [22] X. Quan, X. Liu, L. Bo, S. Chen, Y. Zhao, X. Cui, *Water Res.* 38 (2004) 4484.
- [23] Y. Han, X. Quan, S. Chen, H. Zhao, C. Cui, Y. Zhao, *J. Colloid Interf. Sci.* 299 (2006) 766.
- [24] H. Genc-Fuhrman, J.C. Tjell, D. McConchie, *Environ. Sci. Technol.* 38 (2004) 2428.
- [25] K.P. Singh, D. Mohan, S. Sinha, G.S. Tondon, D. Gosh, *Ind. Eng. Chem. Res.* 42 (2003) 1965.
- [26] X.T. Liu, X. Quan, L.L. Bo, S. Chen, Y.Z. Zhao, *Carbon* 42 (2004) 415.
- [27] S. Brunauer, L.S. Deming, W.E. Deming, E. Teller, *J. Am. Chem. Soc.* 62 (1940) 1723.
- [28] B.K. Pradhan, N.K. Sandle, *Carbon* 37 (1999) 1323.
- [29] G.S. Miguel, S.D. Lambert, N.J.D. Graham, *Water Res.* 35 (2001) 2740.
- [30] F. Julien, M. Baudu, M. Mazet, *Water Res.* 32 (1998) 3414.
- [31] Z. Dega-Szafran, G. Dutkiewicz, Z. Kosturkiewicz, M. Przedwojska, M. Szafran, *J. Mol. Struct.* 649 (2003) 257.
- [32] L.M. Ng, P. Li, *Surf. Sci.* 342 (1995) 359.
- [33] S. Biniak, G. Szymanski, J. Siedlewski, A. Swiatkowski, *Carbon* 35 (1997) 1799.
- [34] A.A. El-Hendawy, *Carbon* 41 (2003) 713.